DALTON
FULL PAPER

Study of the $[CaM(C_3H_2O_4)_2(H_2O)_4]\cdot nH_2O$ [M = Mn, Fe or Co ($n = 0$) and Ni ($n = 2$)] systems: synthesis, structure, spectroscopic and magnetic properties

Izaskun Gil de Muro,[a] Maite Insausti,[a] Luis Lezama,[a] M. Karmele Urtiaga,[b] M. Isabel Arriortua[b] and Teófilo Rojo*[a]

[a] *Departamento de Química Inorgánica, Facultad de Ciencias, Universidad del País Vasco, Apdo. 644, Bilbao 48080, Spain. E-mail: qiproapt@lg.ehu.es*
[b] *Departamento de Mineralogía-Petrología, Facultad de Ciencias, Universidad del País Vasco, Apdo. 644, Bilbao 48080, Spain*

Received 13th July 2000, Accepted 21st July 2000
First published as an Advance Article on the web 7th September 2000

The $[CaM(mal)_2(H_2O)_4]$ (M = Mn, Fe or Co; mal = $C_3H_2O_4$) and $[CaNi(mal)_2(H_2O)_4]\cdot 2H_2O$ compounds have been synthesized and characterized. X-Ray single crystal diffraction analysis was carried out on the $[CaMn(C_3H_2O_4)_2(H_2O)_4]$ and $[CaNi(C_3H_2O_4)_2(H_2O)_4]\cdot 2H_2O$ complexes. The $[CaM(C_3H_2O_4)_2(H_2O)_4]$ (M = Fe or Co) compounds are considered to be isostructural to the former one. The structures consist of three-dimensional networks of metal ions co-ordinated by malonate ligand acting as bridges. The transition metal and calcium ions exhibit octahedral and eight-co-ordination, respectively. Thermogravimetric studies confirm the presence of both co-ordinated and hydrated water molecules. Spectroscopic measurements show high spin octahedral symmetries for the transition metal ions. Magnetic measurements reveal the presence of weak antiferromagnetic interactions in all compounds.

Introduction

The study of perovskite-related mixed oxides was prompted by the discovery of warm superconductors and the magnetoresistive oxides.[1] It is worth mentioning the existence of mixed valence transition metals in these phases. When the transition ions are incorporated into a crystal lattice along with cations such as calcium the higher valence states can be stabilized at higher temperatures giving rise to Ca–M–O (M = Mn, Fe or Co) mixed oxides with interesting properties.[2]

The synthesis of the mentioned oxides was usually performed by solid state reactions which involve high temperatures and long reaction times. In some cases, thermal decomposition of heterometallic complexes has been discovered as a more advantageous way.[3] This method allows one to prepare metastable or stable phases at lower temperatures containing smaller grain sizes than those obtained from the ceramic method. Although different ligands can be used in the synthesis of these compounds, the carboxylate ligands have been used exhaustively to complex the transition metal ions. In this sense, different compounds containing edta, oxalate, tartrate and malonate have been synthesized and used as precursors.[4,5]

The chemistry of heteronuclear complexes involving carboxylate bridging ligands has been investigated exhaustively aided by a wide variety of physical techniques such as electronic spectroscopy, susceptibility measurements and EPR spectroscopy.[6] The malonate ligand, in the bis chelating co-ordination mode, has been shown to be a useful tool for connecting different metals and transmitting different magnetic interactions. In this way, ferromagnetically or antiferromagnetically coupled dimers and alternating chains have been obtained.[7,8]

In this paper, we present the synthesis and characterization of the $[CaM(mal)_2(H_2O)_4]$ (M = Mn, Fe or Co; mal = $C_3H_2O_4$) and $[CaNi(mal)_2(H_2O)_4]\cdot 2H_2O$ compounds. Magnetic measurements indicate the presence of weak antiferromagnetic interactions. Thermal decompositions of the compounds give rise to mixed oxides in the case of manganese and iron precursors.

Experimental

Materials

Manganese(II) nitrate, cobalt(II), iron(II) and nickel(II) chlorides, calcium chloride and malonic acid were purchased from Aldrich Co., sodium carbonate from Merck. All were used without further purification.

Synthesis

To a solution of 2.5 mmol of disodium malonate, previously formed from 2.5 mmol (0.2601 g) of malonic acid neutralized with sodium carbonate, the corresponding chloride of the transition metal (1.0 mmol) was added. The mixture was maintained with stirring for 30 minutes, and then an equimolecular amount of calcium chloride (0.1470 g) added. The mixture was allowed to stand for two hours after which the addition of ethanol (3 ml) yielded polycrystalline powders of all phases. They were filtered off and washed with ethanol–water. The $[CaM(C_3H_2O_4)_2(H_2O)_n]$ (M = Mn, Fe, Co or Ni) compounds were obtained, hereinafter denoted CaMn, CaFe, CaCo and CaNi, respectively. For the iron complex a closed system with a nitrogen atmosphere was employed in order to stabilize the Fe^{2+} ion. For the manganese and nickel compounds, prismatic colourless and green single crystals, respectively, were obtained in diffusion devices. In the case of the other cations, attempts to obtain single crystals have been unsuccessful. Found (calc.)%: for $C_6H_{12}CaMnO_{12}$, C, 19.0(19.4); H, 2.9(3.2); Ca, 10.8(10.7); Mn, 15.0(14.8); for $C_6H_{12}CaFeO_{12}$, C, 18.9(19.3); H, 2.8(3.2); Ca, 10.6(10.7); Fe, 14.5(15.0); for $C_6H_{12}CaCoO_{12}$, C, 18.9(19.2); H, 3.0(3.2); Ca, 10.7(10.6); Co, 15.40(15.7); for $C_6H_{16}CaNiO_{14}$, C, 17.2(17.5); H, 3.8(3.9); Ca, 9.5(9.7); Ni, 14.6(14.3).

Thermogravimetric data are in good accordance with the loss of the water molecules present in the complexes, in the 145–245 °C range. For the $[CaNi(C_3H_2O_4)_2(H_2O)_4]\cdot 2H_2O$ compound the process takes place in two steps which correspond to loss of both crystallization and co-ordination water molecules. X-Ray diffraction of the final products yielded the identification of

 DOI: 10.1039/b005661h

$CaMnO_{3-x}$[9] and $Ca_2Fe_2O_5$[10] phases, in both air and nitrogen atmospheres. For the cobalt and nickel compounds the final residue is a mixture of phases.

Physical measurements

Elemental analyses were performed using a Perkin-Elmer 2400 microanalyser. Analytical measurements were carried out in an ARL 3410 + ICP with Minitorch equipment. Diffuse reflectance spectra were registered at room temperature on a Cary 2415 spectrometer in the range 5000–45000 cm^{-1}. ESR spectra were recorded on a Bruker ESP 300 spectrometer equipped with a standard Oxford low-temperature device operating at X and Q bands. The magnetic field was measured with a Bruker BNM 200 gaussmeter, and the frequency determined with a HP5352B-microwave frequency counter. TG measurements were carried out with a Perkin-Elmer System-7 DSC-TGA unit. Crucibles containing 20 mg of sample were heated at 5 °C min^{-1} under dry air and nitrogen. The powder X-ray diffraction (XRD) patterns were taken using a Philips X-PERT diffractometer with Cu-Kα_1 radiation. Data were collected by scanning in the range $5 < 2\theta < 70°$ with increments of 0.02° (2θ).

Crystal structure determination

Prismatic crystals of $[CaMn(mal)_2(H_2O)_4]$ **1** and $[CaNi(mal)_2(H_2O_4)]\cdot 2H_2O$ **2** with approximate dimensions $0.12 \times 0.22 \times 0.38$ and $0.10 \times 0.10 \times 0.30$ mm, respectively, were mounted on glass fibres and transferred to an Enraf-Nonius CAD-4 diffractometer with graphite-monochromated Mo-Kα radiation. The unit cell parameters were determined using 25 reflections in the range 16–28° for both compounds. Data were collected using ω–2θ scans and reduced using Lorentz and polarization corrections. The structures were solved by heavy-atom Patterson methods using the program SHELXS 97,[11] completed using Fourier difference synthesis, and refined using SHELXL 97.[12] The structures were refined using isotropic thermal parameters prior to the refinement of anisotropic thermal parameters for all the atoms. Hydrogen atom positions were not calculated crystallographically. The geometric calculations were performed with PARST[13] and BONDLA[14] and molecular illustrations were drawn with CRYSTAL MAKER.[15] Details of the data collection and structure refinement can be found in Table 1. Selected bond distances and bond angles are given in Tables 2 and 3.

CCDC reference number 186/2101.

See http://www.rsc.org/suppdata/dt/b0/b005661h/ for crystallographic files in .cif format.

Results and discussion

Structural analysis

The structures of $[CaMn(mal)_2(H_2O)_4]$ **1** and $[CaNi(mal)_2(H_2O)_4]\cdot 2H_2O$ **2** can be described as a three-dimensional network of metal ions which are linked by malonate and hydrogen bonds. Two of the co-ordination water molecules are linked to the Ca^{2+} ions and the other two to the transition metal ions. In the nickel compound the additional water molecules are present in the structure as crystallization water. The co-ordination polyhedra of the metal ions for both phases are represented in Fig. 1.

The maganese(II) and nickel(II) ions are octahedrally co-ordinated lying on an inversion centre. There are four oxygen atoms in the equatorial plane O(1), O(1^{iv}), O(3), O(3^{iv}) for manganese and O(2), O(2^{i}), O(3) and O(3^{i}) for nickel. The apical positions are formed by O(2w) and O(2w^{iv}) for CaMn and O(2w^{ii}) and O(2w^{iii}) for CaNi. The average metal–oxygen distances are shorter for the nickel compound than for the manganese one, 2.05 *vs.* 2.16 Å. The distortion around the transition ions has been calculated by quantification of the Muetterties and Guggenberger description.[16] The values

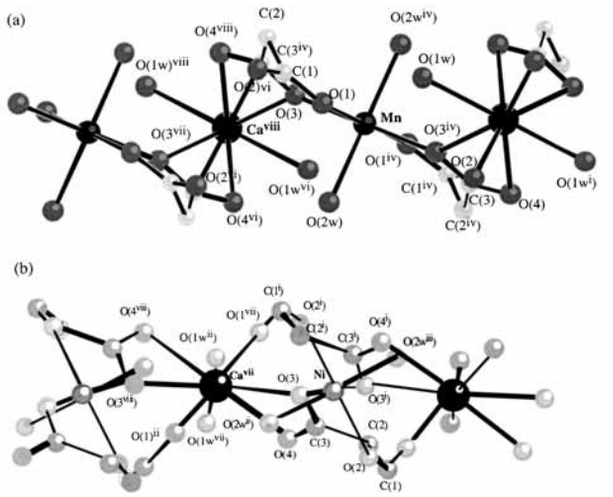

Fig. 1 Schematic representation of the atoms which form the co-ordination polyhedra for the metals in (a) $[CaMn(C_3H_2O_4)_2(H_2O)_4]$ and (b) $[CaNi(C_3H_2O_4)_2(H_2O)_4]\cdot 2H_2O$.

obtained, $\Delta = 0.05$ and 0.035 for **1** and **2** respectively, are indicative of regular octahedra with slight trigonal distortions. The calcium ions, which lie on a binary axis in both structures, are co-ordinated to eight oxygen atoms. Two of them belong to two water molecules and the other six to oxygen atoms from the malonate ligand, forming an irregular polyhedron. For both compounds, the average calcium–oxygen distance is 2.4 Å.

The configuration of the malonate ligands is different in both compounds. In the CaMn compound the chelated malonate ring, Mn–O(3)–C(3^{iv})–C(2)–C(1)–O(1), has an 'envelope' conformation in which only the methylene group is significantly displaced from the ring plane, 0.539(2) Å. For the CaNi compound the malonate rings have a 'boat' conformation in which the methylene group and the nickel(II) ions are displaced from the other atoms. The average C–O distances are 1.253 and 1.260 Å and the average O–C–O angles are 122 and 121.2°, for CaMn and CaNi, respectively.

The O(3) atoms in CaMn link the Mn and Ca ions (Mn–O(3)–Ca^{v} 138.33(6)°) forming perpendicular planes to the [10$\bar{1}$] direction. In these planes the shorter distance Mn $\cdots$ Mn^{vii} is 6.984(5) Å and the distance through the O(3)–Ca^{v}–O(3^{vii}) atoms is 9.518(1) Å. These planes are linked between them along the [10$\bar{1}$] direction *via* hydrogen bonds in which the O(2), O(4) atoms from malonate groups and O(1w), O(2w) from water molecules are linked to the calcium and manganese ions, respectively. The shortest distance between the manganese(II) ions from different planes is 7.62(4) Å. The three-dimensional package in this structure is maintained by the presence of hydrogen bonds.

In the CaNi compound the O(3) atoms link the metal ions forming a Ni–O(3)–Ca^{vii} angle of 141.0(2)°. These connections form zigzag chains extended along the *c* direction (Fig. 2). These chains are linked between them by malonate bridges (Ni–O(2)–C(1)–O(1)–Ca), forming the three-dimensional network. The shortest distance Ni $\cdots$ Ni^{ix} through the chain is 6.637 Å and along O(3)–Ca^{vii}–O(3)^{viii} is 9.264(3) Å. In this structure the oxygen atoms from the water molecules form hydrogen bonds maintaining the three dimensional package.

In the case of $[CaM(mal)_2(H_2O)_4]$ (M = Fe or Co) high quality crystals were not obtained. X-Ray diffraction patterns of the microcrystalline products were recorded in the 2θ range between 5 and 70°. Indexation of the diffraction profile and refinement of the cell parameters were made by FULLPROF (pattern matching analysis)[17] on the basis of the space group *C*2/*c* and the cell parameters found for the CaMn phase.

Table 1 Data collection and structure refinement of $[CaMn(mal)_2(H_2O)_4]$ **1** and $[CaNi(mal)_2(H_2O)_4]\cdot 2H_2O$ **2**

Formula	$C_6H_{12}CaMnO_{12}$	$C_6H_{16}CaNiO_{14}$
M/g mol^{-1}	371.18	416.80
System	Monoclinic	Orthorhombic
Space group	$C2/c$	$Pbcn$
a/Å	14.086(2)	8.921(2)
b/Å	7.488(1)	11.935(5)
c/Å	13.273(3)	13.274(5)
β/°	118.68(2)	
Z	4	8
V/Å^3	1228.2(4)	1413.3(7)
T/°C	20	20
λ/Å	0.71069	0.71069
μ/mm^{-1}	1.556	1.810
Unique data	1794	2062
Observed data	1437	1166
$R(R')$	0.027 (0.063)	0.05 (0.0936)

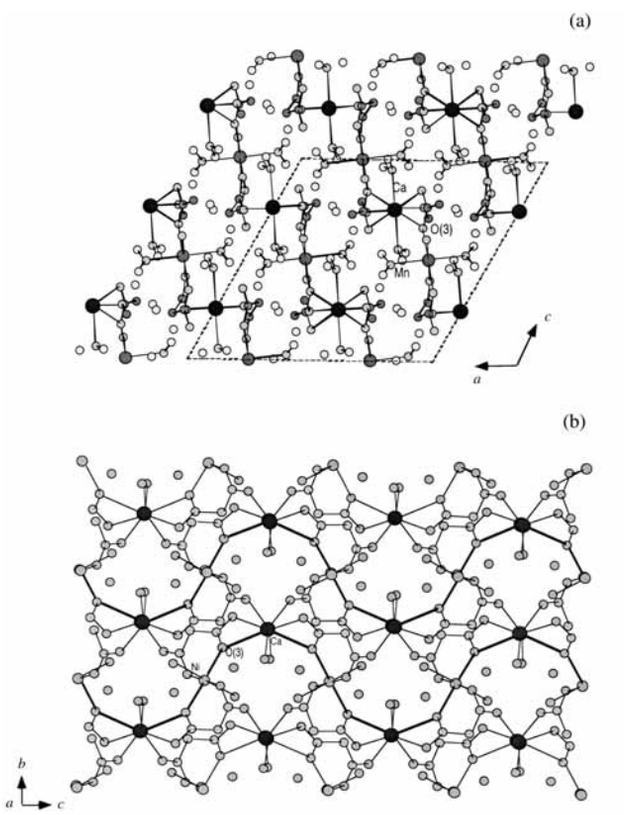

Fig. 2 Schematic representation of (a) $[CaMn(C_3H_2O_4)_2(H_2O)_4]$ in the [0 1 0] direction and (b) $[CaNi(C_3H_2O_4)_2(H_2O)_4]\cdot 2H_2O$ in the bc plane.

The parameters obtained are in Table 4. From these data we consider the three phases to be isostructural.

IR and UV-visible spectroscopies

The most useful information provided by the IR spectra performed on the mentioned compounds is related to the carboxylate bands. In the case of malonic acid a band is observed at 1730 cm^{-1} which is shifted for the present compounds to 1590 cm^{-1}. This fact is indicative of co-ordination of all the carboxylate groups to the metal ions. This band appears together with the antisymmetric $\nu_{asym}(OCO^-)$ vibration, the bands corresponding to the symmetric $\nu_{sym}(OCO^-)$ vibration being localized in the 1330–1388 cm^{-1} range. Taking into account the relative position of the antisymmetric $\nu_{asym}(OCO^-)$ and symmetric $\nu_{sym}(OCO^-)$ vibration bands, the bonding between the metal and the ligand must be through bridges in all compounds.[18] Finally, the bending vibration corresponding to the δ(C=O) group is observed in the 1220–1300 cm^{-1} range, for all compounds.

Reflectance spectra for the $[CaM(C_3H_2O_4)_2(H_2O)_4]$ (M = Fe or Co) and $[CaNi(C_3H_2O_4)_2(H_2O)_4]\cdot 2H_2O$ compounds have been recorded. In the case of the cobalt compound the positions of the bands appear at $\tilde{\nu}_1 = 8000$, $\tilde{\nu}_2 = 15600$ and $\tilde{\nu}_3 = 20000$ cm^{-1} which have been assigned to the $^4T_{1g} \longrightarrow {}^4T_{2g}(F)$, $^4A_{2g}(F)$ and $^4T_{1g}(P)$ transitions. Considering an octahedral model we obtain $Dq = 913$ cm^{-1} and $B = 875$ cm^{-1} which are in good agreement with those observed for cobalt(II) ions in octahedral geometries. For the CaFe compound the band

Table 2 Selected bond distances (Å) and angles (°) with e.s.d.s in parentheses for $[CaMn(mal)_2(H_2O)_4]$

Mn–O(3)	2.143(1)	Ca–O(2)	2.378(1)
Mn–O(1)	2.188(1)	Ca–O(1w)	2,405(1)
Mn–O(2w)	2.192(1)	Ca–O(4^{ii})	2.460(1)
O(1)–C(1)	1.257(2)	Ca–O(3^{ii})	2.616(1)
O(2)–C(1)	1.251(2)	C(2)–C(3)	1.514(2)
C(1)–C(2)	1.519(2)	C(3)–O(4)	1.245(2)
C(3)–O(3)	1.260(2)		
O(1w^i)–Ca–O(1w)	146.42(7)	O(1)–Mn–O(2w^{iv})	91.33(6)
O(1w)–Ca–O(4^{iii})	125.26(5)	O(3)–Mn–O(2w)	89.34(6)
O(4^{ii})–Ca–O(4^{iii})	101.07(7)	O(2)–Mn–O(2w^{iv})	180.0
O(2^i)–Ca–O(3^{ii})	94.91(5)	O(3^{iv})–Mn–O(3)	180.0
O(1w^i)–Ca–O(3^{ii})	77.11(5)	O(3)–Mn–O(1)	83.85(5)
O(4^{ii})–Ca–O(3^{ii})	50.65(4)	O(2)–C(1)–C(2)	116.7(1)
O(4^{iii})–Ca–O(3^{ii})	76.27(5)	O(1)–C(1)–C(2)	119.6(1)
O(2^i)–Ca–O(3^{iii})	153.63(4)	C(3)–C(2)–C(1)	115.9(1)
O(1w^i)–Ca–O(3^{iii})	128.24(4)	O(3)–C(3)–C(2)	121.1(1)
O(4)–C(3)–O(3)	120.6(1)	O(2)–C(1)–O(1)	123.7(1)

Symmetry codes: (i) $-x, y, \frac{1}{2} - z$; (ii) $-x, 1 - y, \frac{1}{2} - z$; (iii) $x, 1 - y, z$; (iv) $\frac{1}{2} - x, \frac{3}{2} - y, 1 - z$.

Table 3 Selected bond distances (Å) and angles (°) with e.s.d.s in parentheses for $[CaNi(mal)_2(H_2O)_4]\cdot 2H_2O$

Ni–O(2)	2.063(3)	Ca–O(1)	2.384(4)
Ni–O(3)	2.039(3)	Ca–O(1w)	2.409(4)
Ni–O(2w^{ii})	2.066(4)	Ca–O(4^v)	2.454(4)
O(1)–C(1)	1.246(6)	Ca–O(3^v)	2.593(3)
O(2)–C(1)	1.264(6)	C(2)–C(3)	1.510(7)
C(1)–C(2)	1.517(7)	C(3)–O(4)	1.248(6)
		C(3)–O(3)	1.280(6)
O(2)–Ni–O(3)	89.1(1)	O(3)–Ni–O(3^i)	180.0
O(2)–Ni–O(2w^{ii})	92.7(1)	O(3)–Ni–O(2w^{iii})	91.8(1)
Ni(1)–O(3)–Ca^{vii}	141.0(2)	O(4^v)–Ca–O(1w)	125.1(1)
O(1)–Ca–O(1^{iv})	94.5(2)	O(1)–Ca–O(4^v)	76.5(1)
O(1w^{iv})–Ca–O(1w)	92.4(2)	O(1)–Ca–O(4^{vi})	82.2(1)
O(4^v)–Ca–O(4^{vi})	148.4(2)	O(3^v)–Ca–O(1w^{iv})	73.2(1)
O(1)–Ca–O(1w)	92.9(1)	O(3^v)–Ca–O(4^v)	51.4(1)
O(1)–Ca–O(3^v)	82.6(1)	Ni–O(2)–C(1)	123.7(3)
O(2)–C(1)–O(1)	122.3(5)	O(4)–C(3)–O(3)	120.2(4)
O(2)–C(1)–C(2)	120.2(4)	O(4)–C(3)–C(2)	119.4(5)
O(1)–C(1)–C(2)	117.5(4)	O(3)–C(3)–C(2)	120.4(4)

Symmetry codes: (i) $-x + 1, -y + 1, -z$; (ii) $x + \frac{1}{2}, -y + \frac{1}{2}, -z$; (iii) $-x + \frac{1}{2}, y + \frac{1}{2}, z$; (iv) $-x, y, -z + \frac{1}{2}$; (v) $x - \frac{1}{2}, -y + \frac{1}{2}, -z$; (vi) $-x + \frac{1}{2}, -y + \frac{1}{2}, z + \frac{1}{2}$; (vii) $-x + \frac{1}{2}, -y + \frac{1}{2}, z - \frac{1}{2}$.

Table 4 Crystallographic data for the $[CaM(C_3H_2O_4)_2(H_2O)_4]$ (M = Mn, Fe or Co) compounds

	CaMn[a]	CaFe	CaCo
a/Å	14.086(2)	13.961(2)	13.879(2)
b/Å	7.488(1)	7.53(1)	7.504(1)
c/Å	13.273(3)	13.487(4)	13.338(3)
β/°	118.68(2)	119.6(1)	119.05(1)
V/Å^3	1228.2(4)	1232.88	1214.28
Space group	$C2/c$	$C2/c$	$C2/c$

[a] Data obtained from single crystal experiments.

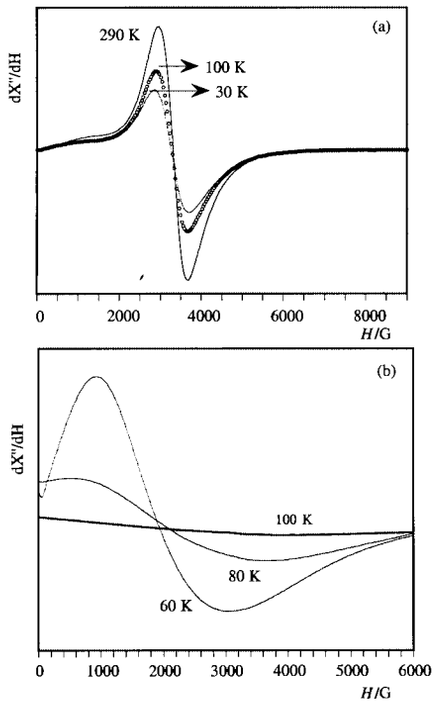

Fig. 3 X-Band ESR spectra of (a) $[CaMn(C_3H_2O_4)_2(H_2O)_4]$ at 290, 100 and 30 K and (b) $[CaCo(C_3H_2O_4)_2(H_2O)_4]$ at 100, 80 and 60 K.

corresponding to the $^5T_g \longrightarrow {}^5E_g$ transition is split in two (10600 and 8700 cm^{-1}), due to the Jahn–Teller distortion of the ^5E_g energy level. From the position of these bands a value of $(8/3)d\sigma = 1900\ cm^{-1}$ (where $(8/3)d\sigma$ is the splitting of the ^5E_g term) was calculated. This fact is indicative of the presence of a slight distortion around the metal ion in this compound. For CaNi the bands that appear at $\tilde{\nu}_1 = 9100$, $\tilde{\nu}_2 = 13900$ and $\tilde{\nu} = 25300\ cm^{-1}$ have been assigned to the three allowed transitions $^3A_{2g} \longrightarrow {}^3T_{2g}$, $^3T_{1g}(F)$ and $^3T_{1g}(P)$. The spin forbidden transitions $^3A_{2g} \longrightarrow {}^1E_g$ and $^1T_{2g}$ were also observed at $\tilde{\nu}_4 = 15400$ and $\tilde{\nu}_5 = 22700\ cm^{-1}$, respectively. The *Dq* and Racah parameters, calculated by fitting the experimental frequencies by an energy level diagram for octahedral d^8 systems, are $Dq = 910\ cm^{-1}$, $B = 950$ and $C = 4050\ cm^{-1}$, values usually found for octahedrally co-ordinated nickel(II) compounds.[19]

ESR and magnetic properties

The X-band ESR spectra of polycrystalline samples of $[CaM(C_3H_2O_4)_2(H_2O)_4]$ (M = Mn or Co) have been recorded in the temperature range 4–300 K. For the CaFe compound no signal was observed due to the presence of Fe^{2+} ions. The spectra for the CaMn compound at different temperatures are represented in Fig. 3(a). Isotropic signals have been observed in all cases, being broader and showing more intensity with decreasing temperature. This fact is unusual and could be explained by the presence of dipolar interactions which would be more significant than the exchange ones at low temperatures. In this case, the behaviour observed for Mn^{II} ($S = 5/2$) is very similar to that for rare-earth-metal ions with high spin moments.[20] The spectra for the CaCo compound at different temperatures are shown in Fig. 3(b). Broad and isotropic signals appear at room temperature, being narrower at low temperatures. The spectrum at 4 K shows the characteristics of a rhombic *g* tensor, $g_1 = 6.52$, $g_2 = 4.103$ and $g_3 = 2.008$, values which are in good accordance with those of a Co^{2+} ion in an octahedral geometry.

Magnetic measurements for all the compounds were carried out in the temperature range 1.8–300 K. The $\chi_m T$ and $\chi_m{}^{-1}$ *vs. T* curves for the CaMn, CaFe and CaCo compounds are represented in Fig. 4. The $\chi_m{}^{-1}$ *vs. T* curves show a Curie–Weiss behaviour in the range 5–300 K with θ values of −0.21 (CaMn),

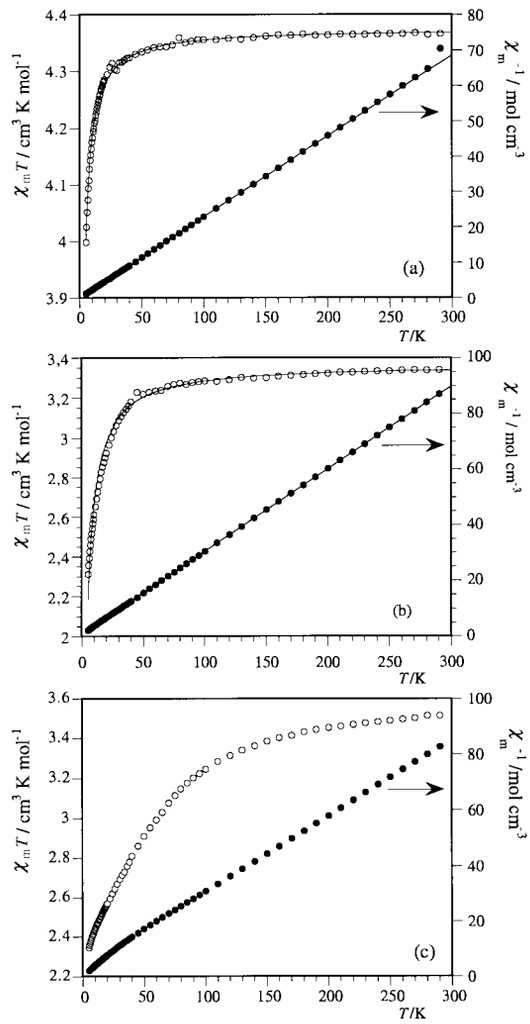

Fig. 4 Thermal evolution of $\chi_m T$ and χ^{-1} for the $[CaM(C_3H_2O_4)_2(H_2O)_4]$ compounds: M = Mn (a), Fe (b) Co (c).

−2.74 (CaFe) and −0.51 K (CaNi) and C_m constants of 4.36, 3.37 and 1.21 $cm^3\ K\ mol^{-1}$, respectively. The decrease for the χ_m *T vs. T* curves when the temperature is lowered together with the θ values indicate the presence of slight antiferromagnetic interactions for these compounds. Taking into account the structural features, the magnetic behaviour for the CaMn and CaFe compounds can be described by the expression given by Rushbrooke and Wood for a Heisenberg three dimensional network.[21] The expressions (1) and (2) were deduced taking into

$$\chi_m = (Ng^2\beta^2/kT)\,[1 + 35x + 221.66x^2 + 608.22x^3 + 26049.56x^4 + 210986.5x^5 + 8014980x^6]^{-1} \quad (1)$$

$$\chi_m = (Ng^2\beta^2/kT)\,2[1 + 24x + 108x^2 + 217.6x^3 + 5696.8x^4 + 33730.6x^5 + 825802x^6]^{-1} \quad (2)$$

account the $S = 5/2$ and $S = 2$ values for the manganese(II) and iron(II) ions, respectively, based on the spin Hamiltonian $H = -2J\ \Sigma_{\langle i,j\rangle} S_i S_j$, where *N* is Avogadro's number, β = Bohr magneton, and *k* = Boltzmann constant, and $x = J/kT$.

The best least-squares fit leads to *J*/*k* values of −0.1 K for CaMn and CaFe with $\langle g \rangle$ values of 2 and 2.11, respectively. In the case of the CaNi compound it was not possible to fit the experimental data by the model described because of the weakness of the magnetic interactions.

For the CaCo compound the data at high temperatures ($T > 60$ K) can also be fitted by a Curie–Weiss law with $\theta = -13.45$ K and $C_m = 3.68\ cm^3$ K per mol of metal ion (Fig. 4c). In this case, the continuous decrease of the $\chi_m T$ curve with

decreasing temperature must be ascribed to the presence of antiferromagnetic exchange interactions, and the effect of the spin–orbit coupling ($\lambda = -170$ cm^{-1} for free Co^{2+} ion)[22] which leads to an effective spin $S = 1/2$ for the system at low temperatures (<30 K). This latter effect is qualitatively similar to those of the antiferromagnetic interactions, making it difficult to distinguish the contributions of these two effects to the whole magnetic behaviour of this compound.

Concluding remarks

The $[CaM(C_3H_2O_4)_2(H_2O)_4]\cdot nH_2O$ (M = Mn, Fe, Co ($n = 0$) or Ni ($n = 2$)) complexes have been synthesized and characterized. The structures of $[CaMn(C_3H_2O_4)_2(H_2O)_4]$ and $[CaNi(C_3H_2O_4)_2(H_2O)_4]\cdot 2H_2O$ consist of three-dimensional networks of metal ions co-ordinated by malonate ligand bridges, where the manganese and nickel ions adopt an octahedral co-ordination. The $[CaM(C_3H_2O_4)_2(H_2O)_4]$ (M = Fe or Co) complexes are considered to be isostructural to the former one. Magnetic measurements reveal the presence of weak antiferromagnetic interactions in all of them. In the cases of CaMn and CaFe a Heisenberg three-dimensional model has been used for explaining the magnetic behaviour. For the cobalt compound the effect of the spin–orbit coupling is similar in magnitude to the antiferromagnetic exchange interactions. A detailed study of the thermal decomposition of the complexes is being performed in order to obtain different mixed oxides.

Acknowledgements

This work has been carried out with the financial support of the Dirección General de Investigación Científica y Técnica (Project PB97-0622) and the Universidad del País Vasco/Euskal Herriko Unibertsitatea (Project 169.310-EB006/98). I. G. M. also thanks the Spanish Government for a Doctoral Fellowship.

References

1 S. Jin, T. H. Tiefel, M. McCormack, R. A. Fastnacht, R. Ramesh and L. H. Chen, *Science*, 1994, **264**, 413; R. von Helmolt, J. Wecker, B. Holzapfel, L. Schultz and K. Samwer, *Phys. Rev. Lett.*, 1993, **71**, 2331.
2 H. S. Horowitz and J. M. Longo, *Mater. Res. Bull.*, 1978, **13**, 1359; S. Aasland, H. Fjellvag and B. C. Hauback, *Solid State Commun.*, 1997, **101**, 187.
3 W. E. Rhine, R. B. Hallock, W. M. Davis and W. Wong-Ng, *Chem. Mater.*, 1992, **4**, 1208.
4 M. Insausti, R. Cortés, M. I. Arriortua, T. Rojo and E. H. Bocanergra, *Solid State Ionics*, 1993, **63–65**, 351.
5 J. García-Jaca, J. I. R. Larramendi, M. Insausti, M. I. Arriortua and T. Rojo, *J. Mater. Chem.*, 1995, **5**, 1995; I. Gil de Muro, F. A. Mautner, M. Insausti, L. Lezama, M. I. Arriortua and T. Rojo, *Inorg. Chem.*, 1998, **37**, 3243.
6 M. Insausti, J. L. Pizarro, L. Lezama, R. Cortés, E. H. Bocanegra, M. I. Arriortua and T. Rojo, *Chem. Mater.*, 1994, **6**, 707.
7 N. J. Ray and B. J. Hathaway, *Acta Crystallogr.*, *Sect. B*, 1982, **38**, 770; D. Chattopadhyay, S. K. Chattopadhyay, P. R. Lowe, C. H. Schwalbe, S. K. Mazumder, A. Rana and S. Ghosh, *J. Chem. Soc.*, *Dalton Trans.*, 1993, 913.
8 S. M. Saadeh, L. T. Kathleen, J. W. Kampf, W. E. Hatfield and V. L. Pecoraro, *Inorg. Chem.*, 1993, **32**, 3034.
9 H. S. Horowitz and J. M. Longo, *Mater. Res. Bull.*, 1978, **13**, 1359.
10 Powder Diffraction File, Card No 19-222. Joint Committee on Powder Diffraction Standards, Swarthmore, PA, 1995.
11 G. M. Sheldrick, SHELXS 97, Program for the Solution of Crystal Structures. University of Göttingen, 1997.
12 G. M. Sheldrick, SHELXL 97, Program for the Refinement of Crystal Structures, University of Göttingen, 1997.
13 M. Nardelli, PARST, *Comput. Chem.*, 1983, **7**, 95.
14 J. M. Stewart (Editor), *The X-ray System*, Technical Report TR-446 of the Computer Science Center, University of Maryland, College Park, Maryland, 1976.
15 D. C. Palmer, CRYSTAL MAKER, Cambridge University Technical Services, Ltd., 1996.
16 E. L. Muetterties and L. J. Guggenberger, *J. Am. Chem. Soc.*, 1974, **96**, 1748.
17 J. Rodriguez-Carvajal, FULLPROF, *Physica B*, 1992, **192**, 55.
18 K. Nakamoto, *Infrared and Raman Spectra of Inorganic and Coordination Compounds*, 5th edn., John Wiley & Sons, New York, 1997.
19 A. B. P. Lever, *Inorganic Electronic Spectroscopy*, Elsevier Science, Amsterdam, 1984.
20 A. Abragam and B. Bleaney, *Electron Paramagnetic Resonance of Transition Ions*, Oxford University Press, Oxford, 1986.
21 G. S. Rushbrooke and P. Wood, *J. Mol. Phys.*, 1963, **6**, 409.
22 T. M. Dunn, *Trans. Faraday Soc.*, 1961, **57**, 1441.